Galactic and Cosmic Type Ia SN rates: is it possible to impose constraints on SNIa progenitors?

I. Bonaparte, ^{1*} F. Matteucci, ^{1,2,3} , S. Recchi, ⁴, E. Spitoni¹, A. Pipino⁵, V. Grieco¹

Department of Physics, Trieste University, Via Valerio 2, 34100, Trieste

- ² INAF, Via G.B. Tiepolo 11, 34100 Trieste
- ³ INFN, Via Valerio 2, 34100, Trieste
- ⁴ Institute for Astrophysics, University of Vienna, Türkenschanzstrasse 17, 1180, Vienna, Austria
- ⁵Institut fur Astronomie, ETH Zurich, CH-8093 Zurich, Switzerland

Released 2013 Xxxxx XX

ABSTRACT

We compute the Type Ia supernova rates in typical elliptical galaxies by varying the progenitor models for Type Ia supernovae. To do that a formalism which takes into account the delay distribution function (DTD) of the explosion times and a given star formation history is adopted. Then the chemical evolution for ellipticals with baryonic initial masses 10^{10} , 10^{11} and $10^{12}M_{\odot}$ is computed, and the mass of Fe produced by each galaxy is precisely estimated. We also compute the expected Fe mass ejected by ellipticals in typical galaxy clusters (e.g. Coma and Virgo), under different assumptions about Type Ia SN progenitors. As a last step, we compute the cosmic Type Ia SN rate in an unitary volume of the Universe by adopting several cosmic star formation rates and compare it with the available and recent observational data. Unfortunately, no firm conclusions can be derived only from the cosmic SNIa rate, neither on SNIa progenitors nor on the cosmic star formation rate. Finally, by analysing all our results together, and by taking into account previous chemical evolution results, we try to constrain the best Type Ia progenitor model. We conclude that the best progenitor models for Type Ia SNe are still the single degenerate model, the double degenerate wide model, and the empirical bimodal model. All these models require the existence of prompt Type Ia supernovae, exploding in the first 100 Myr since the beginning of star formation, although their fraction should not exceed 15-20% in order to fit chemical abundances in galaxies.

Key words: Supernovae – Galaxy evolution– Cosmology.

INTRODUCTION

The study of the mechanisms of supernova (SN) explosions as well as the analysis of their nucleosynthesis products are two key ingredients for understanding the chemical evolution of galaxies. Type Ia supernovae are thought to be the main contributors to the chemical enrichment in iron in the universe and they have also a significant influence on the early and late evolution of galaxies. In elliptical galaxies, in fact, after the occurrence of the galactic wind and the end of the star formation, they are the only SNe occuring. They contribute to eject continuously energy and iron which eventually will reach the intracluster medium (ICM). Type Ia SNe are also used to track the Hubble law and therefore they are fundamentally important in cosmology.

Therefore, the description of the evolution of the SN

Ia rate, in galaxies and in a unitary volume of the universe (cosmic rate), is a crucial information for galaxy evolution and cosmology. The computation of the Type Ia SN rate is related to the nature of the progenitor systems, which unfortunately are still poorly known. The observed features of SNe Ia suggest that these objects may originate from the thermonuclear explosion of CO white dwarfs (WD) of Chandrasekhar mass and the two theoretical main scenarios which have been proposed so are: a) the Single Degenerate (SD) scenario and b) the Double Degenerate (DD) scenario. Recently, it has been suggested also a double detonation in sub-Chandrasekhar masses as a possible mechanism for explaining some of the SNe Ia. In fact, in the last years it has became more and more evident the existence of a variety of Type Ia SNe. Here we will analyze only the classical DD and SD scenarios (see Hillebrandt et al. 2013 for a recent review on all possible scenarios).

2 I. Bonaparte et al.

which the primary component has mass in the range (2 - $8)M_{\odot}$ while the secondary component is a non-degenerate companion, a red giant or a main sequence star (e.g. Whelan & Iben 1973), that has mass in the range $(0.8-8)M_{\odot}$. The lower limit, in the range of masses, is due to the fact that the only systems of interest are those capable of generating a Type Ia SN in a Hubble time to explain the existence of SNe Ia in ellipticals. The upper limit instead is imposed by the fact that single stars with masses $M > 8M_{\odot}$ ignite carbon in a non-degenerate core and do not end their lives as CO WDs. When the secondary star evolves and fills its Roche lobe, the WD accretes material. Thanks to the accretion of matter, via mass transfer from the non-degenerate companion, the primary star reaches the Chandrasekhar mass and explodes. For many years the only suggested explosion mechanism was C-deflagration, but recently it has been suggested that in SD scenario SNe explode via a detonation, after deflagration has been initiated. On the other hand, for the DD scenario the explosion occurs via a prompt detonation or a double detonation (e.g. Pakmor et al. 2013). One of the limitations of the SD scenario is that the accretion rate should be defined in a quite narrow range of values. To avoid this problem, Kobayashi & al. (1998) had proposed a similar scenario, based on the model of Hachisu & al. (1999), where the companion can be either a red giant or a main sequence star, but including a metallicity effect which suggests that no Type Ia systems can form for [Fe/H] < -1.0 dex. This is due to the development of a strong radiative wind from the C-O WD which stabilizes the accretion from the companion, and allowing the WD to reach the Chandrasekhar limit for a wide binary parameter space than the previous scenario. This scenario will not be considered here since models of galactic chemical evolution (e.g. Matteucci & Recchi, 2001) have demonstrated that the SN Ia rate in the Galaxy reaches a maximum when [Fe/H]= -1.0 dex, thus making the long delay due to the metallicity effects unrealistic.

In the original DD scenario the binary system is composed by two CO WDs that, because of the emission of gravitational wave radiation, lose angular momentum and merge achieving the Chandrasekhar mass (e.g. Iben & Tutukov 1984) and explode as mentioned above. The progenitor masses are defined in the range $(5-8)M_{\odot}$ to ensure two WDs of $0.7M_{\odot}$ and then reach the Chandrasekhar mass. The time of the explosion is the lifetime of the secondary star plus the time necessary to merge. The validity of this scenario requires that the two CO WDs have an initial separation less than $3R_{\odot}$, condition that can be reached by means of two different precursor systems: a close binary and a wide binary system. The two scenarios differ for their efficiency of the common envelope phase during the first mass transfer, and therefore for the separation attained at the end of the first common envelope phase. The analysis of the SN Ia rates in the past years has been the subject of several works, as the pioneering works of Greggio & Renzini (1983), Iben & Tutukov (1984), Tornambé & Matteucci (1986), Matteucci & Greggio (1986), and of the most recent works like those of Matteucci & Recchi (2001), Strolger & al. (2004), Greggio (2005), Mannucci & al. (2006), Pritchet & al. (2008), Totani & al. (2008), Valiante & al. (2009). An extensive review on the subject can be found in Maoz & Mannucci (2012). We aim at testing various distributions of explosion times and also different star formation histories for elliptical galaxies.

In fact, once established the nature of the SN Ia progenitors, the Type Ia SN rate is the convolution of the distribution of the explosion times, usually called the delay time distribution function (DTD), with the star formation rate (SFR) of the studied galaxy. The adopted DTDs, which describe the rate at which SNe Ia explode as a function of time in a simple stellar population (a starburt), refer to the single degenerate model (white dwarf plus red giant companion) and to the double degenerate model (two white dwarfs) as well as to empirical DTDs, as suggested by various authors. A large convergence is found for an empirical DTD proportional to t^{-1} which provides a behavior very similar to that predicted by the double degenerate scenario (see later). The purpose of this work is also the computation of the cosmic Type Ia supernova rates, that is the rate as a function of redshift of Type Ia SN explosions in a unitary volume of the universe. The cosmic Type Ia supernova rate is computed using the same DTDs and different cosmic star formation histories. In this case we need to use a cosmic star formation rate that is usually expressed in $M_{\odot}yr^{-1}Mpc^{-3}$. Such histories are partly derived from a fit of observational data and partly from theoretical models making different assumptions about the number density evolution of galaxies. In fact, in the pure luminosity evolution scenario, the number density of galaxies is considered constant as a function of redshift. In the hierarchical galaxy formation scenario, instead, the number density of galaxies is assumed to change with the cosmic time. Therefore, one can in principle, put constraints on the mechanisms of galaxy formation by comparing theoretical results with data of cosmic star formation rate. In this paper we will compare our predicted cosmic Type Ia SN rates with the latest compilation of data for the SNe Ia. Previous works (Maoz & Gal-Yam, 2004; Forster & al. 2006; Valiante & al. 2009; Maoz & al. 2010) have already tried to infer constraints on SNIa progenitors from the cosmic SNIa rate. In particular, Maoz & al. (2010) studied Type Ia SN rates in clusters of galaxies and concluded that a DTD \propto $t^{-1/2}$ can best reproduce the data. However, no firm conclusions were suggested. One difference with the previous works is that here we test the various DTDs also in the chemical enrichment of the intracluster medium (ICM). The paper is organized as follows: in section 2 we describe how to compute the Type Ia SN rate in galaxies, as well as the different DTD functions for the explosion times. In Sections 3 and 4 we present the results for the Type Ia SN rates in a typical elliptical under different assumptions about the SNIa progenitor models. In Section 5 we show the effects of different DTDs in galaxy models on the predicted Fe and gas mass produced by ellipticals in galaxy clusters. In Section 6 we describe how to compute the cosmic Type Ia SN rate by means of different cosmic star formation rates (CSFRs) and we compare our model results to data. In Section 7 some conclusions are drawn.

2 TYPE IA SN RATE: THE FORMALISM

The Type Ia SN rate, from a theoretical point of view, is difficult to derive because of the uncertainty in the nature of progenitors. Assuming that the SD scenario is valid, the SN Ia rate can be written as (Greggio & Renzini, 1983):

$$R_{SNIa} = A_{Ia} \int_{M_{Bm}}^{M_{BM}} \varphi(m) \left[\int_{\mu_{Bmin}}^{0.5} f(\mu_{B}) \psi(t - \tau_{m2}) d\mu_{B} \right] dm$$
(1)

where:

- $\psi(t-\tau_{M2})$ is the SFR at the time of the birth of the binary system.
- A_{Ia} is the fraction of binary systems which can give rise to Type Ia SNe only relative to the mass range $(3-16)M_{\odot}$;
- M_{Bm} and M_{BM} are the maximum and minimum total mass of the binary systems able to reproduce a SN Ia explosion. The value of the upper limit $M_{BM}=16M_{\odot}$ is due to the assumption that the more massive system should be made of two stars of $8M_{\odot}$ each. Instead the minimum total mass of the binary system is assumed to be $M_{Bm}=3M_{\odot}$ to ensure that the companion of the WD is large enough to allow the WD with the minimum possible mass ($\sim 0.5M_{\odot}$) to reach the Chandrasekhar mass limit ($\sim 1.44M_{\odot}$) after accretion.
- The function $f(\mu_B)$ is the distribution of the mass fraction of the secondary stars in binary systems, namely, $\mu_B = \frac{M^2}{(M_1 + M_2)}$, with M1 and M2 being the primary and secondary masses of the system, respectively. This function is derived observationally and in the literature it has often been written (see Greggio & Renzini, 1983: Matteucci & Greggio, 1986) using the following expression:

$$f(\mu_B) = 2^{1+\gamma} (1+\gamma)\mu_B^{\gamma},$$
 (2)

for $0 > \mu_B \ge \frac{1}{2}$.

• τ_{M2} is the lifetime of the secondary star and represents the time elapsed between the formation of the binary system and its explosion.

If we analyze the DD model, the supernova rate can be computed in the following way (Tornambé & Matteucci 1986);

$$R_{SNIa} = Cq \int_{M_{min}}^{M_{max}} \varphi(M) \left[\int_{S_{B_{min}}}^{S_{B_{max}}} \Psi(t - \tau_{M2} - \tau_{gw}) dlog S_B \right] dM$$
(3)

where:

- C is a normalization constant;
- $q = \frac{M_2}{M_1} = 1$ is the ratio between the secondary and the primary mass which, in this scenario, is assumed, for simplicity, to be equal to unity;
- \bullet S_B is the initial separation of the binary system at the beginning of the gravitational wave emission;
- τ_{grav} is the gravitational time-delay, that for systems which can give rise to SNe of Type Ia, varies from 10^6 to 10^{10} years and more (Landau & Lifshitz 1962):

$$\tau_{grav} = 1.48 \cdot 10^8 \frac{\left(\frac{S_B}{r_{\odot}}\right)^4}{\left(\frac{M_1}{M_{\odot}}\right) \cdot \left(\frac{M_2}{M_{\odot}}\right) \cdot \left(\frac{M_1}{M_{\odot}} + \frac{M_2}{M_{\odot}}\right)} yr \qquad (4)$$

It is now possible to use a new more general formulation for the SN Ia rate, as proposed by Greggio (2005, G05), in which the Type Ia SN rate is defined like the convolution between:

- i) the distribution of the explosion times of SN Ia progenitors, that is the time delay distribution function (DTD) and characterizes the progenitor model;
- ii) the star formation rate, namely the amount of gas turning into stars per unit time, that usually is expressed in $\frac{M_{\odot}}{2}$.

The peculiarity of this formulation is that it allows us to include any DTD that can represents a different scenarios with respect to the SD and DD:

$$R_{SNIa}(t) = k_{\alpha} \int_{\tau_i}^{min(t,\tau_x)} A_{Ia}(t-\tau)\psi(t-\tau)DTD(\tau)d\tau$$
 (5)

where:

- $A_{Ia}(t-\tau)$ is the fraction of binary systems which can give rise to Type Ia SNe and in principle it can vary in time. In this new formulation A_{Ia} is relative to the whole range of star masses $(0.1-100)M_{\odot}$, not only relative to the mass range $(3-16)M_{\odot}$, as it is in the old formulation. This is unfortunately a free parameter which is fixed by reproducing the present time SN Ia rate.
- The DTD is defined in the range (τ_i, τ_x) and normalized as:

$$\int_{\tau_i}^{\tau_x} DTD(\tau)d\tau = 1 \tag{6}$$

- τ_i is the time at which the first SNe Ia start exploding, namely is the minimum delay time for the occurrence of Type Ia SNe, while τ_x is the maximum delay time;
- k_{α} is the number of stars per unit mass in a stellar generation and contains the IMF. In particular:

$$k_{\alpha} = \int_{M_{I}}^{M_{U}} \varphi(m)dm \tag{7}$$

with $M_L = 0.1 M_{\odot}$ and $M_U = 100 M_{\odot}$.

The IMF is the mass distribution of stars at birth and its most common parameterization is that of Salpeter (1955) which is a simple one-slope power law generally defined in the mass range $(0.1-100)M_{\odot}$

$$\varphi(m) = am^{-(1+x)} \tag{8}$$

where:

• a is the normalization constant derived by imposing that

$$\int_{0.1}^{100} m\varphi(m)dm = 1. \tag{9}$$

In this paper we have analyzed different DTDs, that are: i)the DTD of the SD scenario as proposed by Matteucci & Recchi (2001); ii) the DTD of the wide DD scenario as proposed by Greggio (2005), and four empirical DTDs which are: i) a bimodal DTD proposed by Mannucci & al. (2006); ii) a gaussian DTD proposed by Strolger & al. (2004); iii) two power law DTDs proposed by Pritchet & al. (2008) and Totani & al. (2008). It should be noted that in the literature there are many DTDs calculated by means of detailed binary evolution calculations (e.g. Yungelson & Livio, 2000; Han & Podsiadlowski, 2004; Belczynski et al. 2005; Ruiter & al.

I. Bonaparte et al.

2009; Mennekens & al. 2010; Wang & al. 2010). However, these detailed calculations are not always easy to use for the kind of semi-analytical calculations performed in this paper.

The DTD of the SD scenario

The SD model (Whelan & Iben 1973), as described by Matteucci & Recchi (MR01), is computed adopting the following formalism:

$$DTD(\tau) \propto \widetilde{\phi}(M_2) \frac{dM_2}{dt}$$
 (10)

which corresponds to the SN Ia rate for an instantaneous starburts. The function $\widetilde{\phi}(M_2)$ is the mass function of the secondary component that, for this DTD, is equal to:

$$\widetilde{\phi}(M_2) = 2^{(1+\gamma)} (1+\gamma) M_2^{\gamma} \frac{(M_b^{(-s-\gamma)} - M_B^{(-s-\gamma)})}{(-s-\gamma)}, \quad (11)$$

where s = 1 + x with x being the Salpeter index. The derivative $\frac{dM_2}{dt}$ was obtained adopting the inverse of the formula (Padovani & Matteucci, 1993):

$$\tau(M) = 10^{\frac{1.338 - \sqrt{1.79 - 0.2232(7.764 - \log(M))}}{0.1116}},$$
 (12)

which defines the relation between the stellar mass M expressed in M_{\odot} and the Main Sequence lifetime τ expressed in yr. The values of the parameters we will adopt in this study are $\gamma = 0.5$, s = 2.35, $M_b = max(2M_2, M_{min})$, $M_B = M_2 + 0.5(M_{max}), M_{min} = 3M_{\odot}, M_{max} = 16M_{\odot}.$ The fraction of prompt SNe in this scenario is $\sim 10\%$. It is worth noting that this MR01 DTD behaves like $t^{-1.6}$ at late times, in agreement with the empirical DTD found for galaxy clusters derived by Sand & al. (2012).

The DTD of the DD scenario

The analytic formulation to describe the DTD in the DD scenario was proposed by Greggio (2005). In that paper there is the analytic formulation of the DTD for two different schemes, : i) close DD scheme, in which the close binary evolution leads to a narrow distribution of the separations, so that the initially closest binaries merge in a short time, and the initially widest binaries tend to populate the long τ_{arav} tail of the distribution. In addition, the most massive binaries tend to end up with the smallest final separation, hence merge more quickly. The ii) wide DD scheme, in which the close binary evolution produces a wide distribution of separations and total binary masses, and these two variables are virtually independent. We considered only the wide DD scheme because it is more in agreement with the observations suggesting the existence of Type Ia SNe exploding at the present in elliptical galaxies, which stopped to form stars several Gyrs ago.

$$DTD(\tau) = \int_{\tau_{n,inf}}^{\min(\tau_{n,x},\tau)} n(\tau_n) S^C(\tau,\tau_n) d\tau_n$$

$$for CLOSE DD$$

$$\int_{\tau_{n,i}}^{\min(\tau_{n,x},\tau)} n(\tau_n) S^W(\tau,\tau_n) d\tau_n$$

$$(13)$$

$$for\ CLOSE\ DD$$
 (14)

$$\int_{\tau}^{\min(\tau_{n,x},\tau)} n(\tau_n) S^W(\tau,\tau_n) d\tau_n \tag{15}$$

$$for WIDE DD$$
 (16)

where:

$$S^{C}(\tau, \tau_n) = \frac{(\tau - \tau_n)_g^{\beta}}{\tau_{gw,x}^{(1+\beta_g)} - \tau_{gw,i}^{(1+\beta_g)}}$$
(17)

for
$$\tau_n \leqslant \tau - \tau_{gw,i}$$
 (18)

$$= 0 \text{ for } \tau_n \geqslant \tau - \tau_{gw,i} \tag{19}$$

(20)

$$S^{W}(\tau, \tau_n) = f_{1,2}^{W}(\tau, \tau_n)^{(-0.75 + 0.25\beta_a)}$$
(21)

for
$$\tau_n \leqslant \tau - \tau_{aw,i}$$
 (22)

$$= 0 \text{ for } \tau_n \geqslant \tau - \tau_{gw,i} \tag{23}$$

The functions $S^{C}(\tau, \tau_n)$ and $S^{W}(\tau, \tau_n)$ are $\propto \frac{\partial g(\tau, \tau_n)}{\partial \tau}$ where $g(\tau, \tau_n)$ is the fraction of systems which, having a nuclear delay equal to τ_n have also a total delay shorter

$$\tau_{n,inf} = \tau_{n,i} \quad \text{for} \quad \tau < \tau_{n,i} - \tau_{gw,x}(\tau_{n,i})$$
(24)

$$\tau_n^{\star} \quad \text{for} \quad \tau \geqslant \tau_{n,i} - \tau_{qw,x}(\tau_{n,i})$$
 (25)

 τ_n^* is the solution of the equation $\tau = \tau_n + \tau_{gw,x}(\tau_n)$;

 τ_n is the nuclear lifetime of the secondary;

 τ_i is the absolute minimum delay of SN Ia progenitors;

 $au_{gw} = \frac{0.15A^4}{(m_{1R} + m_{2R})m_{1R}m_{2R}}Gyr$ with A, m_{1R}, m_{2R} respectively the separation and component masses of DD system, in solar units.

Empirical DTDs

2.3.1 $Bimodal\ DTD$

The bimodal DTD proposed by Mannucci & al. (2006) (MVP06) is derived empirically thanks to the observations of supernovae in radio galaxies. The bimodal trend is given by the sum of two distinct functions:

- i) a prompt Gaussian centered at $5 \times 10^7 yr$;
- ii) a much slower function, either another Gaussian or an exponentially declining function.

This DTD describes a situation where a percentage form 35% to 50% of all SNe Ia explode during the first 100 Myr since the beginning of star formation (prompt SNe Ia), while the rest explodes with larger delays as long as the Hubble time and more (tardy SNe Ia). This DTD can be analytically approximated by the following expressions (Matteucci & al. 2006):

$$log DTD(\tau) = 1.4 - 50(log\tau - 7.7)^{2}$$
 for $\tau < 85Myr$ (26)
-0.8 - 0.9 $(log\tau - 8.7)^{2}$ for $\tau > 85Myr$ (27)

This bimodal DTD can be associated to the SD scenario.

2.3.2 Gaussian DTD

The gaussian DTD proposed by Strolger & al. (2004, S04) is derived thanks to the analysis of the data obtained with Hubble Space Telescope. These observations have allowed to discover 42 SNe in the redshift range 0.2 < z < 1.6. As these data span a large range in redshift, they are ideal for testing the validity of Type Ia supernova progenitor models with the distribution of expected delay times. The result suggests that the models that requires a large fraction of prompt SNe Ia poorly reproduces the observed redshift distribution and are rejected at greater than 95% confidence. The conclusion is that Gaussian models best fit the observed data for mean delay times in the range of (2-4)Gyr. The formula of this DTD is:

$$DTD(\tau, t_d) = \frac{1}{\sqrt{2\pi\sigma_{\tau}^2}} e^{\frac{-(\tau - t_d)^2}{2\sigma_{t_d}^2}}$$
(28)

where $\sigma_{t_d} = 0.5t_d$ and t_d is the characteristic delay time, here assumed to be 4 Gyr.

2.3.3 Power law DTDs

The two power law DTDs are proposed by Totani & al. (2008) and Pritchet & al. (2008). The relation relative to these functions is:

$$DTD(\tau) \propto \tau^{\alpha}$$
 (29)

with $\alpha=-1$ in the Totani & al. case, and $\alpha=-0.5$ in the Pritchet & al. case.

The DTD of Totani et al. (2008) was suggested on the basis of faint variable supernovae detected in the Subaru/XMM-Newton Deep Survey (SXDS). The sample used for the definition of this DTD was composed by 65 SNe showing significant spatial offset from the nuclei of the host galaxies having an old stellar population at z $\sim 0.4-1.2$ out of more than 1000 SXDS variable objects. This DTD supports the idea of the DD model (Maoz & Mannucci, 2012). The DTD proposed by Pritchet et al. (2008) instead was obtained by the data derived from the SNLS survey, that is the SuperNova Legacy Survey, (Sullivan & al. 2006).

2.4 Properties of the different DTD functions

All the trends of the six different DTDs analyzed here are reported in Figure 1.

The SD and DD formulations follow from general considerations on the evolutionary behavior of stars in binary systems. Some parameters play a key role in shaping the SD and DD DTDs, most notably:

- (i) the mass range of the secondaries in systems which provide SNe Ia events;
- (ii) the minimum mass of the primary which yields a massive enough CO WD to ensure the explosion;
- (iii) the efficiency of the common envelope process;

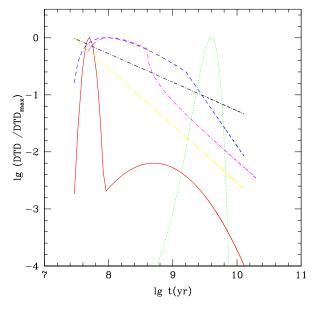


Figure 1. Illustration of the various DTD functions normalized to their own maximum value. The solid red line is the DTD of MVP06; the dashed blue line is the DTD of MR01; the short dashed-dotted magenta line is the DTD of G05; the dotted green line is the DTD of S04; the black short dashed-dotted black line is the DTD of Pritchet & al. (2008); the long dashed yellow line is the DTD of Totani & al. (2008).

- (iv) the efficiency of accretion, for the SD model;
- $(\mathbf{v})\,$ the distribution of the separation, for the DD system at their birth.

The empirical DTDs instead are derived directly from observations.

3 THE PREDICTED TYPE IA RATES IN A TYPICAL ELLIPTICAL

We have predicted the Type Ia SN rate for an elliptical galaxy having a baryonic mass of $10^{11} M_{\odot}$. The assumed cosmology, through all the paper, is the Lambda Cold Dark Matter (Λ CDM) cosmology with $\Omega_M = 0.3$, $\Omega_{\Lambda} = 0.7$ and $H_0 \sim 67 Km s^{-1} Mpc^{-3}$. The SN rate can be computed like the convolution of a given SFR, that it defined as the amount of gas turning into stars per unit time, and a particular DTD, that is the distribution of the explosion times, as shown in eq. (5).

Initially, with the purpose of verifying mostly the dependence of the SN rates on the DTD, we have computed the Type Ia SN rate using only a given SFR and the six different distribution functions studied previously. The trend of this SFR is shown in Figure 2. This SFR is obtained using the Pipino & Matteucci (2004) model applied to an elliptical galaxy of $10^{11} M_{\odot}$ of initial luminous mass, when the SD model for SN Ia progenitors is assumed. In Pipino & Matteucci (2004) model the SFR stops when a galactic wind, triggered mainly by SNe II and Ib,c and partly by SNe Ia, occurs. Other mechanisms exist to devoid galaxies from gas such as ram pressure stripping, tidal stirring and strangula-

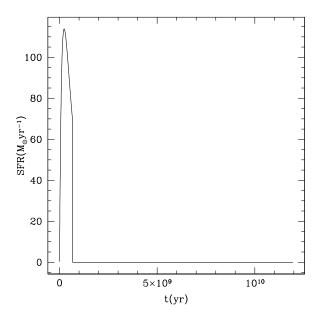


Figure 2. The SFR for an elliptical galaxy of $10^{11} M_{\odot}$. The occurrence of a galactic wind at $t_{GW}=0.67$ Gyr stops the SF.

tion, but we do not consider them here. In any case, there should be a mechanism that quenches star formation in ellipticals and galactic winds seem the most reasonable one. Moreover, as shown by Pipino & Matteucci (2004), galactic winds occurring first in massive than in small ellipticals can very well explain the increase of the $[\alpha/\text{Fe}]$ ratio with galactic mass in ellipticals. Whether such a wind continues for the whole galaxy lifetime is not clear and probably the other mechanisms will be at action as well. However, what matters here is that the gas is soon or later lost into the ICM.

As it can be seen from the Figure 2 the SFR has a simple form given by the Schmidt-Kennicut law, $\psi(t) = \nu \sigma_{gas}^k$, with an efficiency of star formation $\nu = 10 Gyr^{-1}$ and k=1. The SFR is halted by the occurrence of a galactic wind at $t_{GW} = 0.67$ Gyr (see also Valiante & al. 2009).

An important parameter, introduced in the calculation of the rate, is the constant A_{Ia} that represents the fraction of systems which are able to originate a SNe Ia explosion. The value of this constant is calculated a posteriori and it is chosen so as to ensure that the predicted present day SN Ia rate is reproduced. The assumed Type Ia SN rates is given by Cappellaro & al. (1999), that is $0.18 \pm 0.06SNu$, where $1SNu = 1SN/10^{10}L_{\odot B}/century$.

It is necessary to consider that an elliptical galaxy of initial luminous mass of $10^{11} M_{\odot}$ at the present time has a lower luminous mass, because of the presence of the galactic winds. Then the value of the constant A_{Ia} , that we have computed, is relative to a galaxy with a stellar mass of $\sim 3.5 \cdot 10^{10} M_{\odot}$, that is the final mass of the galaxy. As demonstrated by Valiante & al. (2009), to obtain the present time Type Ia SN rate, in units of $SNe \cdot century^{-1}$, for an elliptical with a stellar mass of $3.5 \cdot 10^{10} M_{\odot}$, one should multiply the Cappellaro & al. rate by the blue luminosity predicted for a such galaxy, obtaining a Type Ia SN rate of $0.072SNecentury^{-1}$

Model	A_{Ia}
Mannucci & al. (2006)	0.0053
Matteucci & Recchi (2001)	0.015
Pritchet & al. (2008)	0.00025
Totani & al. (2008)	0.0013
Strolger & al. (2004)	0.028
${ m Greggio}~(2005)$	0.0002

Table 1. Values of the normalization constant $cost_{dtd}$ and A_{Ia} used in the different models. The models refer to the same SF history, the one of Figure 2, but to different DTDs.

(see Valiante & al. 2009). So we have considered this value for the SN Ia rate as reference.

3.1 Properties of different Type Ia SN rates

Figure 3 represents the predicted Type Ia SN rates as functions of redshift for the different DTDs. From this Figure it is possible check that all the curves have a similar trend, except for the rate of S04. This difference in the behaviour of the rate of S04 is due to the fact that this DTD does not contain any prompt SNe Ia and then the peak of this curve is shifted at longer times (several Gyrs). Also the curve for the rate of Pritchet has a particular trend; in fact, it is possible to verify that the peak of this it is much lower compared to all the other curves. The trend of the rate of Totani & al. (2008) is very similar to the rate of Greggio (2005) for wide binaries, in agreement with the conclusions of Totani & al. (2008).

In Table 1 we report the values derived from eq. (5) of the various values of the parameter A_{Ia} , that we considered constant in time, used in the different DTD models in order to obtain a present time SN Ia rate in agreement with observations for a typical elliptical. However, these values for A_{Ia} are only indicative since they change if the history of star formation changes.

4 A MORE SELF-CONSISTENT COMPUTATION OF THE TYPE IA SNE RATE IN A TYPICAL ELLIPTICAL

The above analysis has thus allowed us to emphasize how the DTD function may affect the calculation of the SN Ia rate. With the purpose of having a more precise estimate of the SN Ia rate, we have recalculated the various Type Ia SN rates by adopting the SFR predicted by the chemical evolution model for the various DTDs. In fact, according to the various DTDs, the galactic wind occurs at different times, thus changing the history of SF by truncating it at different times. We recall that a galactic wind occurs when the energy injected into the ISM by SNe equates the gas binding energy. This approach is clearly more self-consistent relative to previous one and it allows us to compute in detail the Fe production in ellipticals, as we will see in Section 5. This fact was not considered in Valiante & al. (2009).

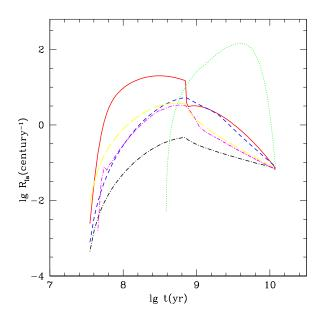


Figure 3. The Type Ia SN rate, as a function of time, for an elliptical galaxy of $10^{11} M_{\odot}$. Symbols are like in Figure 1.

Due to the high similarity of Totani & al. (2008) DTD and that of Greggio (2005) for wide binaries, we will present since now on only the model with the Totani et al. (2008) DTD ($\propto t^{-1}$).

4.1 Star Formation Rates

The histories of star formation dictated by the various DTDs are shown in Fig. 4: one can immediately see how the only SFR that predicts the occurrence of the galactic wind before $\sim 0.67 Gyr$, that is the value relative to the previous SFR relative to the DTD of MR01 (SD scenario), is the SFR relative to the bimodal DTD of Mannucci & al. (2006). In this model, in fact, the birth of a galactic wind occurs at $\sim 0.46 Gyr$, due to the larger number of prompt Type Ia SNe in this DTD. All the other SFRs are lasting for a longer time. On the other hand, the system in which the galactic wind occurs latest is the one related to Pritchet & al. (2008) DTD; in this system, in fact, the SFR vanishes at $\sim 2.64Gyr$, because of the absence of prompt Type Ia SNe. In this case, a large fraction of the Fe produced by Type Ia SNe remains trapped into stars. In the SFR with Totani & al. (2008) DTD the galactic wind occurs at $\sim 1.6 Gyr$, while the galactic wind time obtained with S04 is $\sim 1.75 Gyr$.

The values predicted by the different models for the occurrence of the galactic wind, the total number of SNe Ia exploded during the Hubble time, and the total mass of Fe they produced, are shown in Table 2. The total mass of Fe produced by SNe Ia has been computed by assuming that each SNIa produces $0.6M_{\odot}$ of Fe (Iwamoto & al. 1999).

4.2 Type Ia SN rates

The results of the Type Ia SN rates that we have obtained by exploiting the SFRs determined by the different DTDs are reported in Fig. 5. Clearly the Type Ia SN rates so derived

Model	t_{GW} (Gyr)	SNIa	$M_{Fe} \ ({ m M}_{\odot})$
Mannucci & al. (2006)	0.46	$2.12\cdot 10^8$	$1.27\cdot 10^8$
Matteucci & Recchi (2001)	0.67	$1.47\cdot 10^8$	$8.80 \cdot 10^{7}$
Pritchet & al. (2008)	2.64	$1.5\cdot 10^7$	$9.00\cdot 10^6$
Totani & al. (2008)	1.60	$4.74\cdot 10^7$	$2.84\cdot 10^7$
Strolger & al. (2004)	1.75	$1.68\cdot 10^9$	$1.00\cdot 10^9$

Table 2. Values of the t_{GW} , number of SNe Ia, e total mass of Fe produced by SNeIa ($M_{Fe}(M_{\odot})$) in the different models for a typical elliptical, as described in the text.

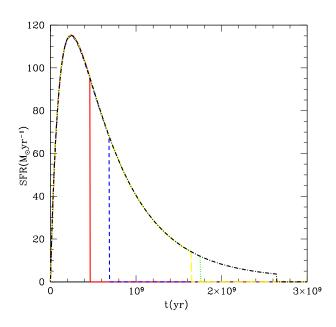


Figure 4. Illustration of the SFR, as a function of time, for an elliptical galaxy of $10^{11} M_{\odot}$. As one can see, the shape of the SFR is the same for all the cases but the SFR is truncated at different times in the different cases. Symbols are like in Figure 1.

present differences relative to those of Figure 3 and they are due to the different duration of the star formation in the various cases. Different DTDs influence differently the onset of the galactic wind, as we have discussed before, and therefore the behaviour of the Type Ia SN rate. Moreover, the value of the constant A_{Ia} undergoes some changes. Varying the SFR, in fact, it is again necessary to ensure that the rate calculated is able to reproduce the current value by introducing the appropriate value of this constant. For the computation of the amount of Fe ejected into the ICM, that we will discuss in the next section, is the time of the occurrence of the galactic wind which influences the amount of Fe remaining trapped in stars versus the amount of Fe which can be ejected into the ICM (namely, all the Fe produced after SF has stopped).

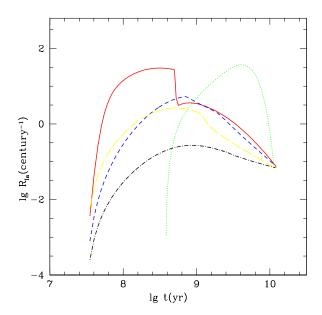


Figure 5. Illustration of the different Type Ia SN rates, as a function of time, for an elliptical galaxy of $10^{11} M_{\odot}$. Symbols are like in Figure 1.

5 CHEMICAL ENRICHMENT OF THE ICM WITH DIFFERENT DTDS

As a test for the different DTDs, we computed the expected Fe enrichment in galaxy clusters. In particular, we considered only two clusters: Virgo and Coma, taken as prototypes of a poor and a rich cluster respectively. The method we adopted is similar to that of Matteucci & Vettolani (1988), Matteucci & Gibson (1995), and Pipino & al. (2002), where the masses produced in the form of Fe and total gas by ellipticals of different masses were integrated over the mass function of the clusters. We remind that the main results of these previous papers were that the Fe mass in clusters is easily reproduced whereas the total gas mass ejected by galaxies is far lower than observed. The logic conclusion from that was that most of the gas in clusters is primordial. We find the same result here. However, here we are interested in comparing the total Fe masses produced by ellipticals evolving with different DTDs. We have considered only four DTDs: i) the MR01 DTD, ii) the Mannucci & al. DTD, iii) the Totani & al. DTD which is similar to the DTD relative to the DD wide scenario, and iv) the S04 DTD. We did not include the Pritchett DTD since it is clear from Table 2 that it predicts a very low number of SNe Ia and therefore of Fe to be ejected into the intracluster medium (ICM). In Table 3 we show the masses of Fe and gas, ejected into the ICM by ellipticals of baryonic masses 10^{10} , 10^{11} , and $10^{12} M_{\odot}$. The chemical evolution model adopted is the one described in Section 2: the assumed efficiencies of star formation are $3Gyr^{-1}$, $10Gyr^{-1}$, and $20Gyr^{-1}$ for 10^{10} , 10^{11} , and $10^{12}M_{\odot}$, respectively (see Pipino & Matteucci, 2004).

In the first column of Table 3 is indicated the DTD adopted in the chemical evolution model, in column 2 the initial baryonic mass of the galaxy, in column 3 the ejected total gas (H, He plus heavier elements), in column 4 the total ejected Fe mass.

Table 3. Masses ejected into the ICM by ellipticals in clusters

-			
DTD	\mathcal{M}_G	${ m M}_{gas}(M_{\odot})$	${ m M}_{Fe}(M_{\odot})$
Mannucci	10^{10}	2.26×10^{9}	8.24×10^{6}
	10^{11}	1.08×10^{10}	3.69×10^7
	10^{12}	8.32×10^{10}	3.30×10^8
Totani	10^{10}	9.66×10^{8}	1.94×10^6
	10^{11}	7.13×10^{9}	1.39×10^7
	10^{12}	6.00×10^{10}	1.22×10^8
-			
Matteucci & Recchi	10^{10}	1.12×10^{9}	2.40×10^7
	10^{11}	1.04×10^{10}	3.25×10^{8}
	10^{12}	8.62×10^{10}	3.05×10^{9}
Strolger & al.	10^{10}	1.37×10^{9}	4.31×10^7
	10^{11}	8.44×10^{9}	4.61×10^{8}
	10^{12}	7.54×10^{10}	4.79×10^{9}

Clearly, the Fe masses ejected into ICM in the different cases are quite different, because the time at which the galactic wind occurs and SF stops is different in different galaxies. In Tables 4 and 5 we show the total mass of Fe and gas ejected into the ICM after integrating the single galactic contributions over the cluster mass function for Virgo and Coma, respectively. In the same Tables are shown the observed values for M_{qas} and M_{Fe} . For Virgo we assumed the following values of the parameters necessary for the integration (see Matteucci & Vettolani, 1988 for details): M/L=10(typical mass to light ratio of ellipticals), $\alpha = -1.25$ (slope of the Schechter (1976) function), f = 0.43 (fraction of ellipticals in the cluster), $n^* = 20$ (cluster richness), and $M_* = -22$ (absolute magnitude of the galaxy at the break of the luminosity function). For Coma we have adopted: $M/L = 10, \ \alpha = -1.25, \ f = 0.82, \ n^* = 115, \ M_* = -22.$ The assumed Hubble constant is $67 \text{ kmsec}^{-1} \text{Mpc}^{-1}$.

From Tables 4 and 5 we can see that in the Mannucci & al. DTD case, the Fe ejected into the ICM is less than in the SD case (MR01 DTD): this is because the number of prompt Type Ia SNe, in this DTD, is quite large and 50% of all SNe Ia explode inside 100 Myr, before the galactic wind. As a consequence, most of the Fe produced by these SNe will be incorporated into stars at variance with what happens for the DTDs of MR01 and Totani, where the fraction of prompt SNe is much lower. However, in the Totani DTD($\propto t^{-1}$)

Table 4. Virgo: integrated gas and Fe masses

DTD	${\rm M}_{gas}(M_{\bigodot})$	${\rm M}_{Fe}(M_{\odot})$
Mannucci	6.16×10^{11}	2.33×10^{9}
Totani	3.42×10^{11}	6.90×10^{8}
Matteucci & Recchi	4.45×10^{11}	1.29×10^{10}
Strolger & al.	4.55×10^{11}	2.12×10^{10}
Observed values	$2\cdot 10^{13}$	$1.6\cdot10^{10}$

Table 5. Coma: integrated gas and Fe masses

DTD	${\rm M}_{gas}(M_{\bigodot})$	${\rm M}_{Fe}(M_{\odot})$
Mannucci	6.75×10^{12}	2.56×10^{10}
Totani	3.74×10^{12}	7.56×10^{9}
Matteucci & Recchi	4.88×10^{12}	1.41×10^{11}
Strolger & al.	4.99×10^{12}	2.33×10^{11}
Observed values	$(4.4 \pm 1.2) \cdot 10^{14}$	$3.1\cdot10^{11}$

, although the number of prompt SNe is lower, the total number of SNe Ia is also lower than in the other cases. So, the smallest amount of Fe ejected into the ICM is the one from Totani's DTD and is not enough to explain the Fe observed in both clusters. On the other hand, the integrated values for Fe in the MR01 DTD and in the S04 DTD produce Fe masses in agreement with observations. It is worth noting that the S04 DTD predicts the smallest masses of total gas ejected into the ICM; this is due to the fact that the galactic winds in ellipticals occur latest with this DTD. Therefore, the amount of residual gas at the time of the wind is lower than in the other cases. If we compute the Fe abundance in the ICM by dividing the total Fe mass predicted for each cluster by the observed mass of gas we obtain, for the MR01 DTD, values in very good agreement with observations ($\sim 0.3 Fe_{\odot}$, Renzini, 2004): in particular, for Virgo we obtain: $Fe_{Virgo} \sim$ $0.4-0.5Fe_{\odot}$ and for Coma $Fe_{Coma} \sim 0.2-0.3Fe_{\odot}$, having assumed the solar Fe abundance by Asplund & al. (2009) $(Fe_{\odot} \sim 1.34 \cdot 10^{-3} \text{ by mass}).$

6 THE COSMIC TYPE IA SN RATE

Another goal that we have set is to test the six different DTDs, previously analyzed, in the computation of the cosmic Type Ia SN rate. The determination of the cosmic Type Ia SN rate, as well as the calculation of the Type Ia SN rate, is obtained as the convolution between the assumed cosmic star formation rate (CSFR) and the DTD function. The CSFR is the star formation rate in a unitary comoving volume of the universe and it is expressed in units of $M_{\odot}yr^{-1}Mpc^{-3}$. For each of the DTD, that we will use, we will adopt five different cosmic star formation rates, that is: i) Cole & al. (2001) modified (see later) CSFR; ii) Madau, Della Valle & Panagia (1998) MDP01 and MDP02 CSFRs; iii) S04 CSFR; iv) Grieco & al. (2012) CSFR. The assumed cosmology, as stated before, is the Lambda Cold Dark Matter (Λ CDM) cosmology.

6.1 The cosmic star formation rate

The physical meaning of the CSFR is of cumulative SFR owing to galaxies of different morphological types present in a unitary comoving volume of the Universe. The CSFR is not a directly measurable quantity and it can be computed only from the measurement of the luminosity density in different wavebands, which are then transformed into star formation rate by a suitable calibration. At high redshift, in fact, it is difficult to distinguish galaxy morphology but it is only possible to trace the luminosity density of galaxies.

6.1.1 Cole & al.(2001) CSFR

The cosmic star formation rate density proposed by Cole & al. (2001) has the form:

$$\dot{\rho}_{Cole} = \frac{a + bz}{1 + (\frac{z}{c})^d} \tag{30}$$

where (a, b, c, d) = (0.0, 0.0798, 1.658, 3.105) and after the correction for the dust extinction are (a, b, c, d) = (0.0166, 0.1848, 1.9474, 2.6316). This parametric fit of the CSFR was obtained thanks to the analysis of the data of Two Micron All Sky Survey (2MASS) Extended Source Catalog and the 2dF Galaxy Redshift Survey. Cole & al. (2001) used these data to estimate the galaxy luminosity function and to infer the total mass fraction in stars. In the computation of this CSFR, Cole & al. (2001) have assumed that no mass goes into forming brown dwarfs and they have multiplied the star formation rate by (1-R) where R is the recycled fraction, as defined in the Simple Model of chemical evolution (Tinsley 1980), they have obtained an estimate of the mass locked up in stars. Here we have done the best fit of all the data on CSFR previously used by Cole & al. (2001) plus some new ones (see Vincoletto & al. 2012 for the data and references). The obtained best fit is very similar to that of Cole & al. (2001) and it is shown in Figure 6 together with the other CSFRs adopted in this paper. We will refer to it as the modified Cole CSFR. For the modified Cole CSFR we have adopted the following parameters: a=0.00904, b=0.1122, c=3.325, d=4.143.

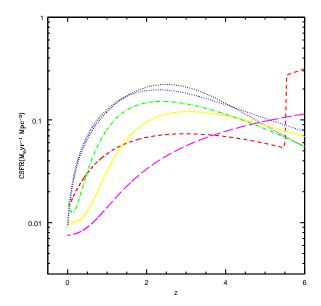


Figure 6. Illustration of the various cosmic star formation history. The dotted blue line is the CSFR of Cole & al. (2001) whereas the black dotted line is the modified Cole CSFR (see text); the solid yellow line is the CSFR of MDP01; the long dashed magenta line is the CSFR of MDP02; the dashed-dotted green line is the CSFR of S04 (2004); the short dashed red line is the CSFR of Grieco & al. (2012).

6.1.2 MDP (1998) CSFR

The two cosmic SFR models MDP01 and MDP02 computed in Madau & al.(1998) are:

$$\dot{\rho}_{MDP01}(t) = a_1 \left[t_9^{a_2} e^{-\frac{t_9}{a_3}} + a_4 (1 - e^{-\frac{t_9}{a_3}}) \right]$$
 (31)

$$\dot{\rho}_{MDP02}(t) = a_1 e^{-\frac{t_9}{a_6}} + a_4 (1 - e^{-\frac{t_9}{a_3}}) + a_5 t_9^{a_2} e^{-\frac{t_9}{a_3}}$$
(32)

where:

 $t_9 = 13(1+z)^{-(\frac{3}{2})}$ is the Hubble time at redshift z;

 $a_1 = 0.049$ in MDP01, $a_1 = 0.336$ in MDP02;

 $a_2 = 5$ in both cases;

 $a_3 = 0.64$ in both cases;

 $a_4 = 0.2$ in MDP01, $a_4 = 0.0074$ in MDP02;

 $a_5 = 0.00197;$

 $a_6 = 1.6$

6.1.3 Strolger & al. (2004) CSFR

This CSFR is given by:

$$\dot{\rho}_{S04}(t) = a_1(t^{a_2}e^{-\frac{t}{a_3}} + a_4e^{\frac{d(t-t_0)}{a_3}})$$
 (33)

where:

 $t_0 = 13.47Gyr$ is the age of the Universe;

 $a_1 = 0.182;$

 $a_2 = 1.260;$

 $a_3 = 1.865;$ $a_4 = 0.071;$

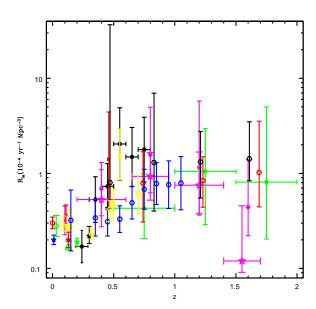


Figure 7. Illustration of the observational data: Barris & Tonry (2006) (black filled hexagons), Dahlen et al. (2004) (magenta filled hexagons), Kuznetsova et al. (2008) (magenta open stars), Poznanski et al. (2007) (green filled hexagons), Cappellaro et al. (1999) (blue open stars), Hardin et al. (2000) (yellow open triangles), Blanc et al. (2004) (green open triangles), Mannucci et al. (2005) (green open hexagons), Magdwick et al. (2003) (magenta filled triangles), Strolger et al. (2003) (red filled hexagons), Neil et al. (2007) (yellow open hexagons), Horesh et al. (2008) (green open stars), Botticella et al. (2008) (black open stars), Tonry et al. (2003) (red filled squares). Neill et al. (2006) (blue filled pentagons), Pain et al. (2002) (yellow filled hexagons), Graur et al. (2011) (red open hexagons), Rodney & Tonry (2010) (blue open hexagons), Li et al. (2010) (red open pentagons), Dilday et al. (2010) (yellow filled stars), Dahlen et al. (2008) (black open hexagons).

These parameters are determined by fitting the collection of measurements of the CSFR of Giavalisco & al. (2004). This CSFR is a model based on a modified version of the parametric form suggested by Madau et al. (1998), taking into account dust extinction.

6.1.4 Grieco & al. (2012) CSFR

To compute the CSFR Grieco & al. (2012) have adopted the following relation:

$$\dot{\rho}_{Grieco} = \sum_{k} \psi_{k}(t) \cdot n_{k}^{\star}(M_{\odot} \cdot yr^{-1} \cdot Mpc^{-3})$$
 (34)

where:

k identifies a particular galaxy type, that is elliptical, spiral or irregular;

 $\psi_k(t)$ represents the history of star formation in each galaxy, tested by model of galactic chemical evolution;

 n_k^* is the galaxy number density, expressed in units of Mpc^{-3} for each morphological galaxy type, and it is been

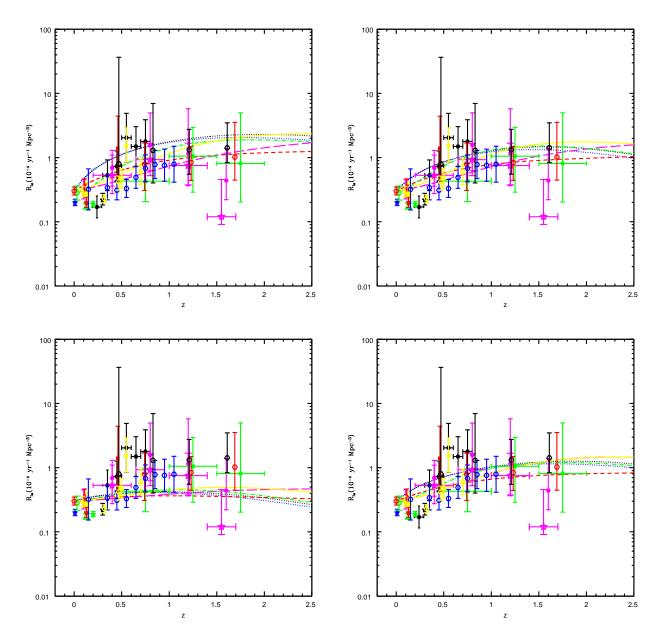


Figure 8. Comparison between model and data. The two top panels are related to the MVP06 DTD, one on the left, and the other to the MR01 DTD plied to the 5 different CSFRs of Figure 6 (the symbols are the same as in Fig.7). In the last two panels there are the Pritchet & al. DTD, on the left, and on the right the Totani & al. DTD, also applied to the 5 CSFRs of Fig.6.

assumed to be constant and equal to the present time one; models assuming number density evolution can be found in Vincoletto & al. (2012).

For the computation of this CSFR Grieco & al. (2012) have assumed that all galaxies started forming stars at the same time, an oversimplified hypothesis but useful to understand the behaviour of the cosmic rates in extreme conditions.

6.1.5 Trend of different CSFRs

To make a comparison between all the CSFR that we analyzed we list all the trends in Figure 6.

Among the five different curves only two have a different

behaviour, that of Grieco & al. (2012) and that of MDP02. The Grieco & al. (2012) CSFR, in fact, shows a quick rise at very high redshift followed by a sharp decline and a following smooth decline until the present time. The rising CSFR for z>5 depends on the fact that in this model all the ellipticals are assumed to be present since the beginning (no number density evolution). On the other hand, the MDP02 CSFR has only one continuous phase of slow growth and it mimics a monolithic collapse scenario. In both CSFRs a Salpeter (1955) IMF is assumed. These two curves therefore do not have the usual trend that is common to the other three curves, that is an initial phase of growth, the reach of a peak and finally a descending phase. All the other mod-

els assume a hierarchical galaxy formation where the most massive objects form later.

6.2 Observational data

The benefit of these new calculations is that, in this case, we can compare the results of our models with a recent compilation of observational data as function of redshift. The data that we have used are reported in Appendix (Tables 6 and 7), where we indicate the references, the redshift and the values of the cosmic SN Ia rate, expressed in $10^{-4} Mpc^{-3}yr^{-1}$. The most recent ones are from Graur & al. (2011) and come from the SubaruDeep Field search. The data with their error bars are also shown in Figure 7.

6.3 Computation of the cosmic Type Ia rate

The computation of the cosmic Type Ia rate is, as already said, similar to the computation of the Type Ia SN rate; so, also in this case, it is necessary to introduce the constant A_{Ia} to reproduce the actual value of the cosmic SN Ia rate. The actual value (z=0) of the cosmic Type Ia rate is $0.301(10^{-4}Mpc^{-3}yr^{-1})$, as proposed by Li & al. (2011).

6.3.1 Properties of the different cosmic Type Ia SN rate

The model results compared to the data are shown in Figures 8, 9 and 10. In Figures 8 and 9, each model was obtained by the convolution between a given DTD and five different CSFRs, shown in Figure 6. These models are compared to the observed cosmic Type Ia SN rate. From this Figure we can see that the models that generally agree with most of the data are unable to reproduce the data of Cappellaro &al. (1999), Blanc & al. (2004). On the other hand, most of the models reproduce the data of Graur & al. (2011), Li & al. (2011) and Rodney & Tonry (2010). Moreover, it is worth noticing that the adopted data suggest a minimum of the cosmic Type Ia SN rate at $z \sim 0.2-0.3$ (see Fig. 7). This is confirmed by a more quantitative analysis. The average SNIa rate for the redshift bin $0 < z \le 0.1$ is 0.273, i.e. it is lower than the present cosmic rate (0.301) determined by Li & al. (2011). The average SNIa rate further decreases in the redshift bins $0.1 < z \le 0.2$ (0.244) and $0.2 < z \le 0.3$ (0.195). Then it starts growing for z > 0.3 (it is 0.448 in the redshift bin $0.3 < z \le 0.4$). None of the adopted combinations of CSFRs and DTDs is able to reproduce this minimum. In order to reproduce it, we should either assume a peculiar CSFR with a minimum at high z (but available data do not corroborate it) or a DTD with a minimum at large delay times (but from a theoretical point of view this is not easy to justify).

Looking at the Figures 8 and 9 it is possible to see how the models computed using the Pritchet & al. (2008) DTD are all too low compared to the data. The same effect seems to be present for the S04 DTD. However, it is very difficult to select a particular DTD and a particular CSFR as the best fit to the data. First of all because of the large error bars present in the data and the different way in which the errors have been computed in different papers. Because of this, any conclusion concerning DTD and CSFR should be

taken with care. Concerning the CSFR, we can see from Figures 8 and 9 that in all models, even in those which are not able to fit very well the data, the curve relative to the modified Cole & al. (2001) CSFR predicts the best trend. With the aim of studying this CSFR more in detail, we made a complementary analysis in which we used only the CSFR of Cole & al. (2001) and the different DTDs. The result obtained is shown in Figure 10. The same considerations made for Figures 8 and 9 hold for this Figure. Although, the modified Cole CSFR is probably the best CSFR since it represents the fit to to the observed CSFR, it is still not possible to extract the best DTD from this diagram. In fact, just looking by eye one can conclude that the DTDs of Pritchett and S04 are too low relative to the average of the data, whereas the DTDs of Mannucci, MR01 and Totani are probably too high. For choosing the best DTD, it is better to rely to chemical evolution results which adopt elemental abundances measured with higher precision. We adopted a fitness test, as described in Calura & al. (2010) (see their eq. 12), to select the best combination DTD/CSFR and the results are shown in Figure 11. From this figure it appears, that the modified Cole and the Grieco & al. (2012) CSFR are the best together with S04, MR01 and Totani DTDs. One can see that in the Figure 11, where the size of the circle is inversely proportional to the fitness function, as defined in Calura & al. (2010). The fact that MR01 and Totani 's DTDs are the best is not surprising since they correspond to the two most popular and tested Type Ia SN scenarios, the SD and the DD ones. However, it is surprising that also the DTD of S04 is good since it is very different from the other two and it does not reproduce the chemical evolution of the solar vicinity (see Matteucci & al. 2009). The abundance patterns in the solar neighbourhood, in fact, demand the presence of some prompt Type Ia SNe and a majority of tardy Type Ia SNe. Therefore, no firm conclusions can be derived from the cosmic Type Ia SN rate, since the uncertainties in the measured rates prevent a reliable analysis relative to the DTDs.

7 CONCLUSIONS

We have computed the Type Ia SN rates in elliptical galaxies of various baryonic masses, under different assumptions about Type Ia SN progenitors. To take into account the different SN Ia progenitors, we adopted different delay time distribution functions (DTDs) describing the distribution of the explosion times as a function of time. We considered both theoretical and empirical DTD functions. The different DTDs have all being normalized to reproduce the present day SNIa rate in typical ellipticals but they contains a different total number of SNeIa and a different proportion of prompt (exploding in the first 100 Myr since the beginning of star formation) and tardy SNe Ia. The bimodal DTD contains $\sim 50\%$ of prompt SNe, the SD DTD (MR01) contains $\sim 13-15\%$, the DD DTD and the DTD $\propto t^{-1}$ (Totani & al. 2008) contain \sim 10%, the DTD $\propto t^{-0.5}$ (Pritchett & al. 2008) contains $\sim 4\%$ and the DTD of S04 contains zero. Then, we have calculated the integrated Fe and gas mass in two galaxy clusters (Coma and Virgo) by means of the models for ellipticals including different DTDs. Finally, we have studied the cosmic Type Ia SN rate by adopting the

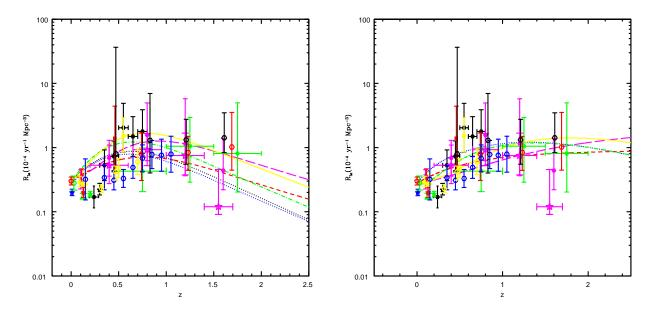


Figure 9. Comparison between model and data. The two panels are related to the S04 DTD and to G05 DTD.

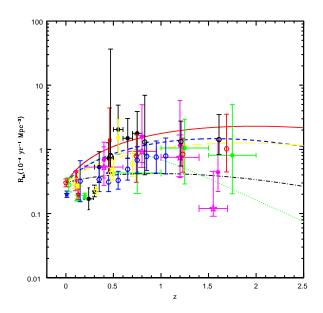


Figure 10. Comparison between the model and the data, relative to the cosmic Type Ia SN rate computed using the modified Cole & al (2001) CSFR and all the DTD. The solid red line is the cosmic Type Ia SN rate of MVP06; the short dashed blue line is the cosmic Type Ia SN rate of MR01; the dotted green line is the cosmic Type Ia SN rate of S04; the short dashed-dotted black line is the cosmic Type Ia SN rate of Pritchet & al. (2008); the long dashed yellow line is the cosmic Type Ia SN rate of G05 is not reported because is identical to the one of Totani & al. (2008)

same DTDs as for the elliptical galaxies and by varying the assumed cosmic star formation rate (CSFR). We considered CSFRs obtained either as bestfits of data or theoretically, and containing different assumptions about galaxy forma-

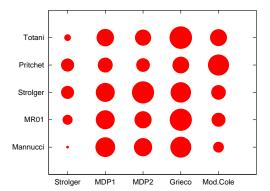


Figure 11. Results of the fitness test for finding the best combination of CSFR and DTD. In the Y axis we report the various DTDs while in the X axis the various CSFRs. The size of the circle is inversely proportional to the calculated fitness function, as defined in Calura & al. (2010), therefore better CSFR/DTD combinations appear as the largest circles.

tion mechanisms. We compared the predicted cosmic Type Ia SN rates with the most recent compilation of data relative to the cosmic Type Ia rate observed up to redshift z = 1.75. We have then compared our model results with observations. It is worth noting that the results of this investigation should integrate those obtained by Matteucci & al. (2009). In that paper we tested the effects of different DTDs on the chemical evolution of the Milky Way and we obtained clear suggestions; in particular, we found that only the SD and DD DTDs together with the bimodal DTD, but with less than 50% prompt Type Ia SNe, can fit the abundance patterns observed in the stars of the Galaxy. Abundance measurements are very accurate these days and certainly more accurate than cosmic SN rate ones. In Matteucci et al. (2009) we also concluded that prompt Type Ia SNe are necessary to reproduce the abundance data.

Our main conclusions can be summarized as follows:

- We have found that a different number of prompt Type Ia SNe affects substantially the time for the occurrence of a galactic wind, which then quenches star formation and gives rise to the passive evolutionary phase for such galaxies. Clearly, the time for a galactic wind influences the amount of Fe locked up in stars as well as that ejected into the ICM. • The best DTD in order to obtain the right amount of Fe in the ICM is the one relative to the single degenerate scenario in the formulation of Greggio & Renzini (1983) and Matteucci & Recchi (2001). The DTD obtained by Totani & al. (2008), which is similar to the DTD of G05 DD wide scenario, does not produce enough Fe to be ejected into the ICM. This DTD, in fact, contains less SNe Ia than the MR01 SD scenario and therefore the galactic wind occurs later. As a consequence of this, the Fe ejected into the ICM is less than in the MR01 SD scenario. The S04 DTD instead produces masses of Fe compatible with observations, but the amount of the total gas ejected is the lowest. This is due to the late galactic winds occurring in galaxies if this DTD is assumed. • The cosmic Type Ia SN rate is not a good tracer of the DTD nor of the CSFR. In spite of the fact that we adopted the largest data set, the observed Type Ia SN rates are still quite uncertain and limited to a redshift $z \leq 1.75$, and the error bars are quite large, especially at high z. We have performed a statistical analysis and found that the best DTDs seems to be those relative to the SD (MR01) and DD (G05) scenarios plus the DTD of S04. This last DTD was in fact deduced from a fit to the observed cosmic Type Ia SN rates. However, given the lack of prompt Type Ia SNe, this DTD does not reproduce correctly the chemical evolution of galaxies, as shown by Matteucci & al. (2006; 2009). In particular, the lack of prompt Type Ia SNe produces a long plateau in the $[\alpha/\text{Fe}]$ ratios in the Galaxy, at variance with observations. The opposite effect is obtained when the bimodal DTD is assumed with 50% of prompt SNe. In this case $\left[\alpha/\text{Fe}\right]$ ratios decrease too steeply with [Fe/H], at variance with observations. The CSFRs adopted here are derived from both hierarchical and monolithic models of galaxy formation; in particular, different assumptions about the galaxy number density evolution underline these cases. In hierarchical models the galaxy number density varies with the cosmic time whereas in monolithic models the galaxy number density is assumed constant (pure luminosity evolution). Moreover, we took into consideration the fit of Cole & al. (2001) of observational data and we also added other points and derived a revised best fit. From our analysis we suggest that the best
- of pure luminosity evolution.

 In summary, taking all of our results together we suggest that the best DTDs are those relative to the SD, DD and bimodal scenarios. All these DTDs contain prompt Type Ia SNe. We also suggest that the ideal number of prompt Type Ia SNe should not exceed 15-20% of the total SNe Ia. However, these results are mainly supported by chemical evolution considerations rather than by the galactic and cosmic Type Ia SN rates. Therefore, the answer to the title of the paper is still rather negative. More precise data on SN

ones to reproduce the cosmic Type Ia SN rate are that derived as a bestfit of observational data (Cole & al. 2001 and

this paper) and a theoretical CSFR derived from chemical evolution models (e.g. Grieco & al. 2012)in the framework

Ia rates in galaxies and as a function of redshift will help in the future to find a more precise answer.

ACKNOWLEDGMENTS

We thank E. Cappellaro for providing the data on the SN cosmic rates. F.M. acknowledges financial support from PRIN MIUR 2010-2011, project "The Chemical and Dynamical Evolution of the Milky Way and Local Group Galaxies, prot. 2010LY5N2T.Finally, we thank an anonymous referee for his/her careful reading of the manuscript and important suggestions.

References

Asplund, M., Grevesse, N., Sauval, A. J., Scott, P., 2009, ARA&A, 47, 481

Barris, B. J. & Tonry, J. L., 2006, 637, 427

Belczynski, K., Bulik, T., Ruiter, A. J., 2005, ApJ, 629, 915

Blanc, G., Afonso, C., Alard, C., Albert, J. N., Aldering, G., Amadon, A., Andersen, J., Ansari, R., 2004, A&A, 423, 881

Botticella, M. T., Riello, M., Cappellaro, E., Benetti, S., Altavilla, G., Pastorello, A., Turatto, M., Greggio, L. & al., 2008, A&A, 479, 49

Calura, F., Recchi, S., Matteucci, F., Kroupa, P., 2010, MNRAS, 406, 1985

Cappellaro E., Evans R., Turatto M., 1999, A&A, 351, 459 Cole S., Norberg P., Baugh C.M., Frenk C.S, Bland-Hawthorn J., Bridges T., Cannon R., Colless M., & al., 2001 MNRAS, 326,255

Dahlen, T., Mobasher, B., Jouvel, S., Kneib, J.-P., Ilbert, O., Arnouts, S., Bernstein, G., Rhodes, J., 2008, AJ, 136, 1361

Dahlen, T., Strolger, L.-G., Riess, A.G., Mobasher, B., Chary, R.-R., Conselice, C.J., Ferguson, H. C., Fruchter, A. S. & al., 2004, ApJ, 613, 189

Dilday, B., Smith, M., Bassett, B., Becker, A., Bender, R., Castander, F., Cinabro, D., Filippenko, A. V. & al., 2010, ApJ, 713, 1026

Dilday, B., Kessler, R., Frieman, J. A., Holtzman, J., Marriner, J., Miknaitis, G., Nichol, R. C., Romani, R., & al., 2008, ApJ, 682, 262

Förster, F. Wolf, C., Podsiadlowski, Ph., Han, Z., 2006, MNRAS, 368, 1893

Giavalisco, M., Dickinson, M., Ferguson, H. C., Ravindranath, S., Kretchmer, C., Moustakas, L. A., Madau, P., Fall, S. M., & al., 2004, ApJ, 600, L103

Graur, O., Poznanski, D., Maoz, D., Yasuda, N., Totani, T., Fukugita, M., Filippenko, A. V., Foley, R. J., 2011, MNRAS, 417, 916

Greggio L. & Renzini A., 1983, A&A, 118, 217

Greggio, L., 2005, A&A, 441, 1055 (G05)

Grieco V., Matteucci F., Meynet G., Longo F., Della Valle M., Salvaterra R., 2012, MNRAS, 423, 3049

Hachisu I., Kato M., Nomoto K., 1999, ApJ, 522, 487

Han, Z., Podsiadlowski, Ph., 2004, MNRAS, 350, 1301

Hardin, D., Afonso, C., Alard, C., Albert, J. N., Amadon,

- A., Andersen, J., Ansari, R., Aubourg, É. & al., 2000, A&A, 362, 419
- Hillebrandt, W., Kromer, M., Röpke, F. K., Ruiter, A. J., 2013, Frontiers of Physics, Vol.8, Issue2, p.116
- Horesh, A., Poznanski, D., Ofek, E. O., Maoz, D., 2008, MNRAS, 389, 1871
- Kobayashi, C., Tsujimoto, T., Nomoto, K., Hachisu, I., Kato, M., 1998, ApJ, 503, 155
- Kuznetsova, N., Barbary, K., Connolly, B., Kim, A. G., Pain, R., Roe, N. A., Aldering, G., Amanullah, R. & al., 2008, ApJ, 673, 981
- Iben I.Jr., Tutukov A.V., 1984, ApJ, 284, 719
- Iwamoto, K., Brachwitz, F., Nomoto, K., Kishimoto, N., Umeda, H., Hix, W. R., Thielemann, F-K, 1999, ApJS, 125, 439
- Landau, L. & Lifschitz, E., 1962, Quantum Mechanics, Pergamon, London
- Li, W., Chornock, R., Leaman, J., Filippenko, A.V., & al., 2011, MNRAS, 412, 1473
- Madau P., Della Valle M., Panagia N., 1998, MNRAS, 297, L17
- Mannucci F., Della Valle M., Panagia N., Cappellaro E. Cresci G., Maiolino R., Petrosian A., Turatto M., 2005, A&A, 433, 807
- Mannucci, F., Della Valle, M., Panagia, N., 2006 MNRAS 370,773.
- Mannucci F., Maoz D., Sharon K., Botticella M.T., Della Valle M., Gal-Yam A., Panagia N., 2008, MNRAS, 383, 1121
- Maoz, D. & Mannucci, F., 2012, PASA, 29, 447
- Maoz, D. & Gal-Yam, A., 2004, MNRAS 347, 951
- Maoz, D., Sharon, K. Gal-Yam, A., 2010, ApJ, 722, 1879
 Madgwick, D., Hewett, P.C., Mortlock, D.J., Wang, L., 2003, ApJ, 599, L33
- Matteucci, F. & Greggio, L., 1986, A&A, 154, 279
- Matteucci F. & Vettolani G., 1988, A&A, 202, 21
- Matteucci, F. & Gibson B.K., 1995, A&A, 304, 11
- Matteucci F. & Recchi S., 2001, ApJ 558, 351)MR01)
- Matteucci F., Panagia N., Pipino A., Mannucci F., Recchi S. Della Valle M., 2006, MNRAS, 372, 265
- Matteucci F., Spitoni E., Recchi S., Valiante R., 2009, A&A, 501, 531
- Mennekens, N., Vanbeveren, D., De Greve, J. P., De Donder, E., 2010, A&A, 515, 89
- Neill, J.D., Sullivan, M., Balam, D., Pritchet, C. J., Howell,
 D. A., Perrett, K., Astier, P., Aubourg, E., & al., 2007,
 THE MULTICOLORED LANDSCAPE OF COMPACT
 OBJECTS AND THEIR EXPLOSIVE ORIGINS. AIP
 Conference Proceedings, Volume 924, p. 421
- Neill, J. D., Sullivan, M., Balam, D., Pritchet, C. J., Howell, D. A., Perrett, K., Astier, P., Aubourg, E. & al., 2006, AJ, 132, 1126
- Minkowski R., 1941, MNRAS, 53, 224.
- Pain, R., Fabbro, S., Sullivan, M., Ellis, R. S., Aldering, G., Astier, P., Deustua, S. E., Fruchter, A. S., & al., 2002, ApJ, 577, 120
- Pakmor, R., Kromer, M., Taubenberger, S., Springel, V., 2013, ApJ, 770, L8
- Pipino, A. & Matteucci, F., Borgani, S., Biviano, A., 2002, NewAstr, 7, 227
- Pipino, A., Matteucci, F., 2004, MNRAS,
- Poznanski, D., Maoz, D., Yasuda, N., Foley, R. J., Doi, M.,

- Filippenko, A. V., Fukugita, M., Gal-Yam, A. & al., 2007, MNRAS, 382, 1169
- Pritchet C.J., Howell D.A., Sullivan M., 2008, ApJ, 683, 25 Porter A.C., Filippenko A.V., 1987, AJ 93, 1372
- Renzini A., 2004, in "Clusters of Galaxies: Probes of Cosmological Structure and Galaxy Evolution", from the Carnegie Observatories Centennial Symposia. Published by Cambridge University Press, as part of the Carnegie Observatories Astrophysics Series. Edited by J.S. Mulchaey, A. Dressler, and A. Oemler, 2004, p. 260.
- Rodney, S.A. & Tonry, J.L, 2010, ApJ, 723, 47
- Rothenflug, R. & Arnaud, M., 1985 A&A, 144, 431
- Ruiter, A. J., Belczynski, K., Fryer, C., 2009, ApJ, 699, 2026
- Sand, D. J., Graham, M. L., Bildfell, C., Zaritsky, D., Pritchet, C., Hoekstra, H., Just, D. W., Herbert-Fort, S. et al., 2012, ApJ, 746, 163
- Salpeter, E.E., 1955, ApJ, 121, 161
- Schechter, P., 1976, ApJ, 203, 297
- Strolger, L.-G., Riess, A., Dahlen, T., Hubble Higher-z Supernova Search Team, GOODS Team, 2003, Bulletin of the American Astronomical Society, Vol. 35, p.1278
- Strolger L., Riess A.G., Dahlen T., Livio M., Panagia N., Challis P., Tonry J.L., Filippenko A.V., & al., 2004, ApJ, 613, 200 (S04)
- Sullivan M., Le Borgne D., Pritchet C.J., Hodsman A., Neill J.D., Howell D.A., Carlberg R.G., Astier P., & al. 2006, ApJ, 648, 868
- Tonry, J. L., Schmidt, B. P., Barris, B., Candia, P., Challis, P., Clocchiatti, A., Coil, A. L., Filippenko, A. V. & al., 2003, ApJ, 594, 1
- Tornambé A., Matteucci F., 1986, MNRAS, 223, 69
- Totani T., Morokuma T., Oda T., Doi M., Yasuda N., 2008, Astronomical Society of Japan, Vol.60, No.6, p.1327
- Valiante R., Matteucci F., Recchi S., Calura F., 2009, New Astronomy, Vol 14, p. 638
- Vincoletto L., Matteucci F., Calura F., Silva L., Granato G., 2012, MNRAS, 421, 3116
- Wang, B., Li, X.-D., Han, Z.-W., 2010, MNRAS, 401, 2729 Whelan, J. & Iben, I.Jr., 1973, ApJ, 186, 1007
- Yungelson, L.R. & Livio, M., 2000, ApJ, 528, 108

Reference	z	SN rate $(10^{-4} Mpc^{-3}yr^{-1})$
Cappellaro & al. (1999)	0.01	0.20 ± 0.059
Hardin & al. (2000)	0.14	$0.22^{+0.17}_{-0.22}$
Pain & al. (2002)	0.55	1.53 ^{+0.28} _{-0.25}
Magdwick & al. (2003)	0.10	0.32 ± 0.15
Strolger & al. (2003)	0.11	0.37 ± 0.10
Tonry & al. (2003)	0.46	1.4 ± 0.5
Blanc & al. (2004)	0.13	$0.14^{+0.05}_{-0.035}$
Dahlen & al. (2004)	0.4	$0.69^{+0.34}_{-0.27}$
Dahlen & al. (2004)	0.8	$1.57^{+0.44}_{-0.25}$
Dahlen & al. (2004)	1.2	$1.15^{+0.47}_{-0.26}$
Dahlen & al. (2004)	1.6	$0.44^{+0.32}_{-0.25}$
Mannucci & al. (2005)	0.03	0.28 ± 0.11
Barris & Tonry (2006)	0.25	$0.17^{+0.17}_{-0.16}$
Barris & Tonry (2006)	0.35	0.53 ± 0.24
Barris & Tonry (2006)	0.45	0.73 ± 0.24
Barris & Tonry (2006)	0.55	2.04 ± 0.38
Barris & Tonry (2006)	0.65	1.49 ± 0.31
Barris & Tonry (2006)	0.75	1.78 ± 0.34
Neill & al. (2006)	0.47	$0.42^{+0.09}_{-0.13}$
Neill & al. (2007)	0.32	0.23 ± 0.06
Neill & al. (2007)	0.50	0.48 ± 0.15
Neill & al. (2007)	0.7	0.60 ± 0.20
Poznanski & al. (2007)	0.75	$0.43^{+0.36}_{-0.32}$
Poznanski & al. (2007)	1.25	$1.05^{+0.45}_{-0.56}$
Poznanski & al. (2007)	1.75	$0.81^{+0.79}_{-0.60}$

Table 6. A compilation of the observational cosmic Type Ia rates at different redshifts up to $z\sim 1.75$.

Reference	\mathbf{z}	SN rate $(10^{-4} Mpc^{-3}yr^{-1})$
Botticella & al. (2008)	0.30	$0.22^{+0.10}_{-0.08}$
Dahlen & al. (2008)	0.47	$0.80^{+1.66}_{-0.27}$
Dahlen & al. (2008)	0.83	$1.30^{+0.73}_{-0.51}$
Dahlen & al. (2008)	1.21	$1.32^{+0.32}_{-0.38}$
Dahlen & al. (2008)	1.61	$0.42^{+0.39}_{-0.23}$
Dilday & al. (2008)	0.09	$0.29^{+0.09}_{-0.07}$
Horesh & al. (2008)	0.2	0.189 ± 0.042
Kuznetsova & al. (2008)	0.4	$0.53^{+0.39}_{-0.17}$
Kuznetsova & al. (2008)	0.8	0.93 ± 0.25
Kuznetsova & al. (2008)	1.2	$0.75^{+0.35}_{-0.30}$
Kuznetsova & al. (2008)	1.55	$0.12^{+0.58}_{-0.119}$
Dilday & al. (2010)	0.12	$0.269^{+0.034}_{-0.030}$
Li & al. (2011)	0	$0.301^{+0.062}_{-0.061}$
Rodney & Tonry (2010)	0.15	0.32 ± 0.32
Rodney & Tonry (2010)	0.35	0.34 ± 0.19
Rodney & Tonry (2010)	0.45	0.31 ± 0.15
Rodney & Tonry (2010)	0.55	0.32 ± 0.14
Rodney & Tonry (2010)	0.65	0.49 ± 0.17
Rodney & Tonry (2010)	0.75	0.68 ± 0.21
Rodney & Tonry (2010)	0.85	0.78 ± 0.22
Rodney & Tonry (2010)	0.95	0.76 ± 0.25
Rodney & Tonry (2010)	1.05	0.79 ± 0.28
Graur & al. (2011)	0.74	$0.79^{+0.33}_{-0.41}$
Graur & al. (2011)	1.23	$0.84^{+0.25}_{-0.28}$
Graur & al. (2011)	1.69	$1.02^{+0.54}_{-0.36}$

Table 7. A compilation of the observational cosmic Type Ia rates at different redshifts up to $z\sim 1.75$.